Induced abundant oxygen vacancies in $Sc_2VO_{5-\delta}$/g-C_3N_4 heterojunction for enhanced photocatalytic degradation of levofloxacin

Jian Feng*, Liyao Zu, Hongrong Yang, Yuanyuan Zheng, Ziying Chen, Wei Song, Ran Zhao, Li Wang, Xia Ran, Bo Xiao

Engineering Research Center for Molecular Medicine, School of Basic Medical Science, Guizhou Medical University, Guiyang 550025, China

* Corresponding author. Tel.: +86 851 88174017
E-mail address: jfeng@gmc.edu.cn (Jian Feng)

Table S1. The peak area percentage of OL, OV and the ratio of OV/OL in SVCs and SV

Sample	OL %	OV %	OV/OL
SV40	45.5	54.5	1.20
SV50	70.4	29.6	0.42
SV60	73.6	26.4	0.36
5%SVC	73.6	26.4	0.36
10%SVC	38.5	61.5	1.60
20%SVC	57.2	42.8	0.75

Table S2. The ratio of OV/OL in 10%SVC samples prepared at different calcination temperature

Sample	OL %	OV %	OV/OL
10%SVC40	43.5	56.5	1.30
10%SVC45	42.2	57.8	1.37
10%SVC50	38.5	61.5	1.60
10%SVC55	41.0	59.0	1.28

Table S3. The pseudo first order k_{app} of photodegradation reaction of MB and RhB over CN, SVCs and SV

Sample	k_{app} (min^{-1}, MB)	k_{app} (min^{-1}, RhB)
CN	0.0171	0.0360
2%SVC	0.0279	0.0758
5%SVC	0.0316	0.0627
10%SVC	0.0432	0.1240
20%SVC	0.0223	0.0574
SV	0.0052	0.0031

Table S4. Comparison of photocatalytic degradation efficiency of MB, RhB and LVX on 10%SVC with various catalysts

Photocatalysts	Reaction Conditions	Removal efficiency %	Reference
10%SVC	80 min, 40 W white LED	MB (98.8%), RhB (99.0%), LVX (89.1%)	this work
g-C_3N_4-CdS	180 min, 500 W Xe-lamp	90.45% (MB)	[1]
MCN/rGOA	80 min, 300 W Xe-lamp	RhB (95.2%)	[2]
g-C_3N_4-ZnO@GA(30%)	120 min, 300 W Xe-lamp	RhB (82.7%)	[3]
hm-CN	120 min, 300 W Xe-lamp	RhB (92.73%), MB (56.95%)	[4]
AgI/$Ag_2Mo_2O_7$	90 min, 300 W Xe-lamp	LVX (64.5%)	[5]
SnTCPP/g-C_3N_4/Bi_2WO_6	140 min, 250 W Xe-lamp	RhB (93.64%), LVX (85.64%)	[6]
SnO_2/BiOCOOH	60 min, 5 W LED (λ = 365 nm)	RhB (98.5%), LVX (85%)	[7]
P_2-Mn_3O_4	10 min, 500 W Xe-lamp	LVX (81.9%)	[8]

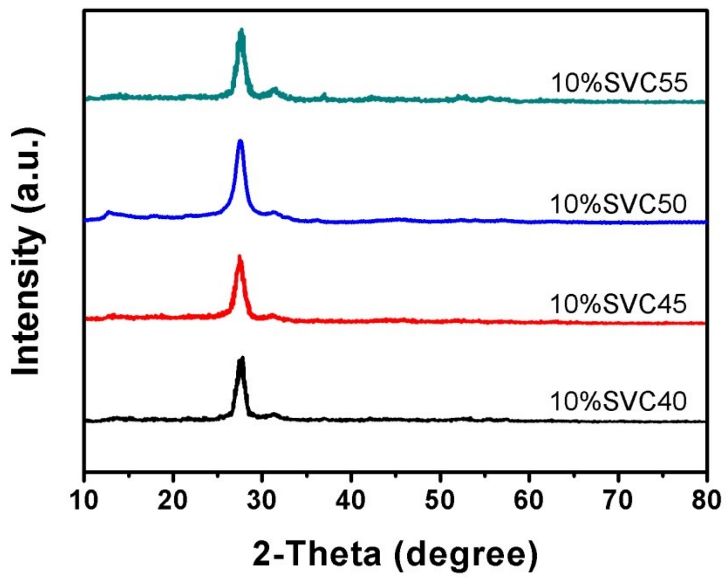

Fig. S1 XRD patterns of 10%SVC samples synthesized with different calcination temperature

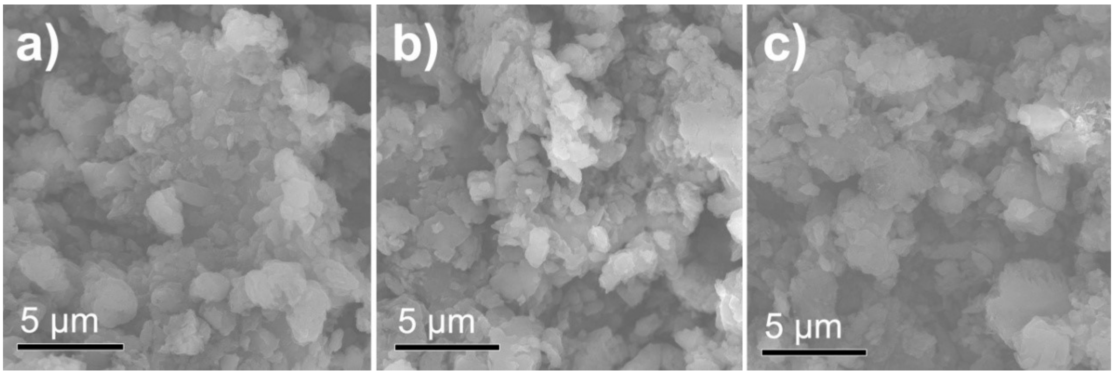

Fig. S2 SEM images of a) 2%SVC, b) 5%SVC and c) 20%SVC

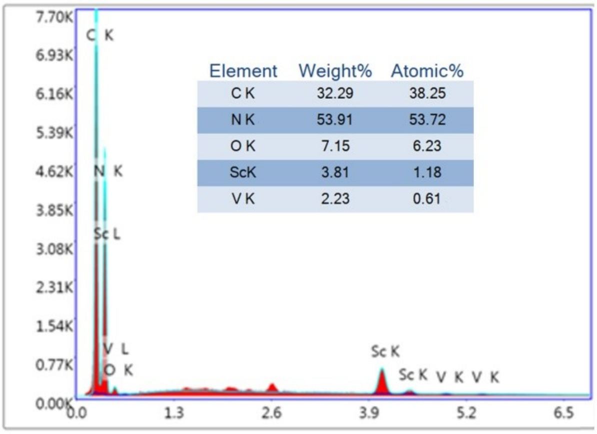

Fig. S3 EDS spectra of 10%SVC

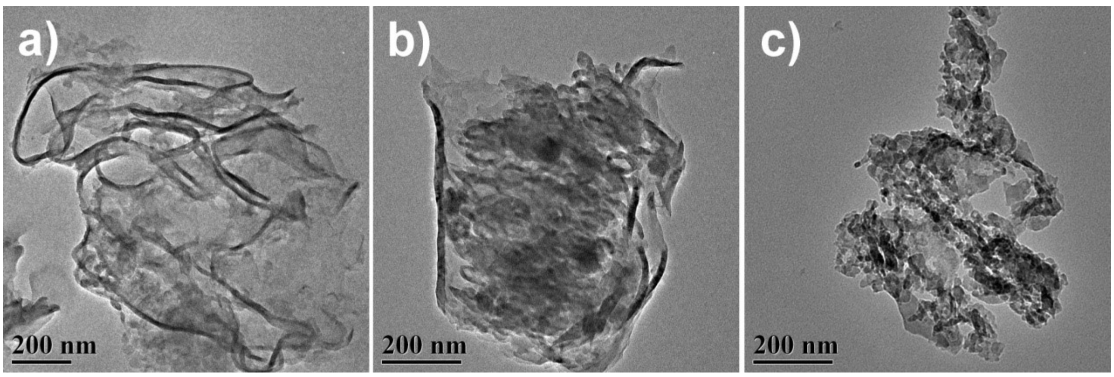

Fig. S4 TEM images of a) 2%SVC, b) 5%SVC and c) 20%SVC

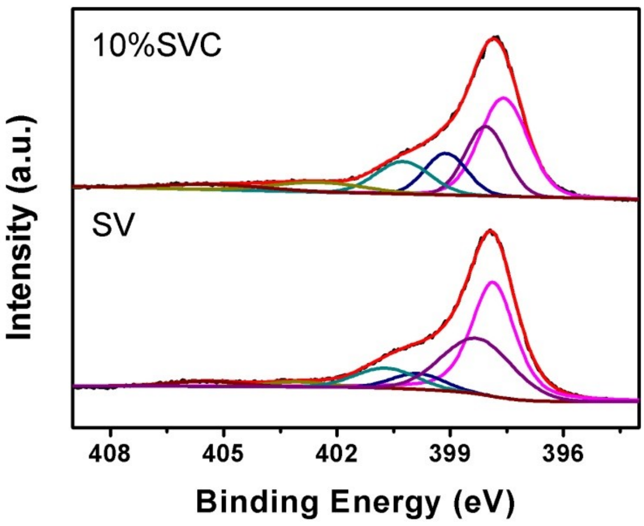

Fig. S5 The Sc2p XPS spectra of 10%SVC and SV

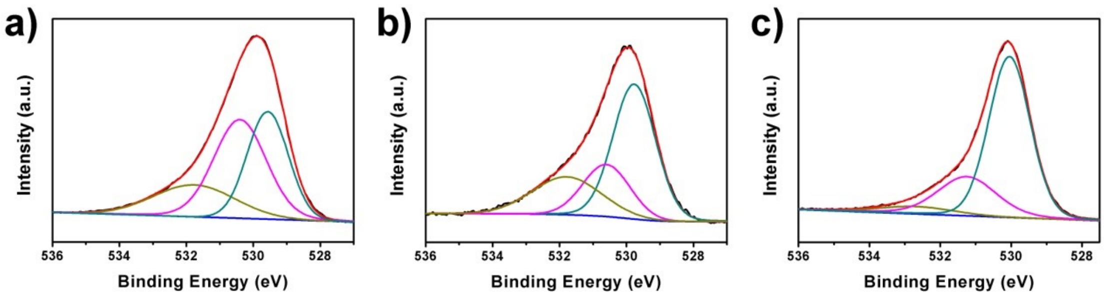

Fig. S6 The O1s XPS spectra of a) SV40, b) SV50 and c) SV60

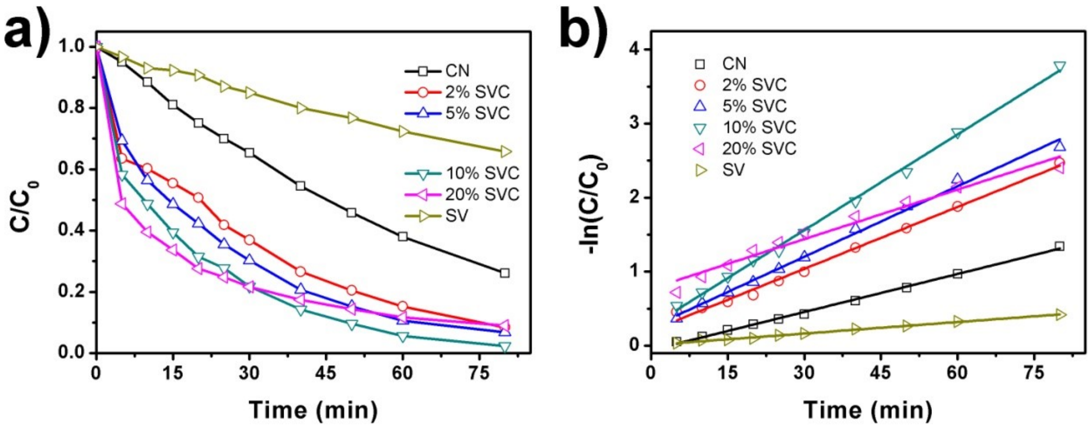

Fig. S7 Photocatalytic degradation of MB over CN, SVCs and SV under visible light irradiation and b) corresponding first-order kinetics fitting plots

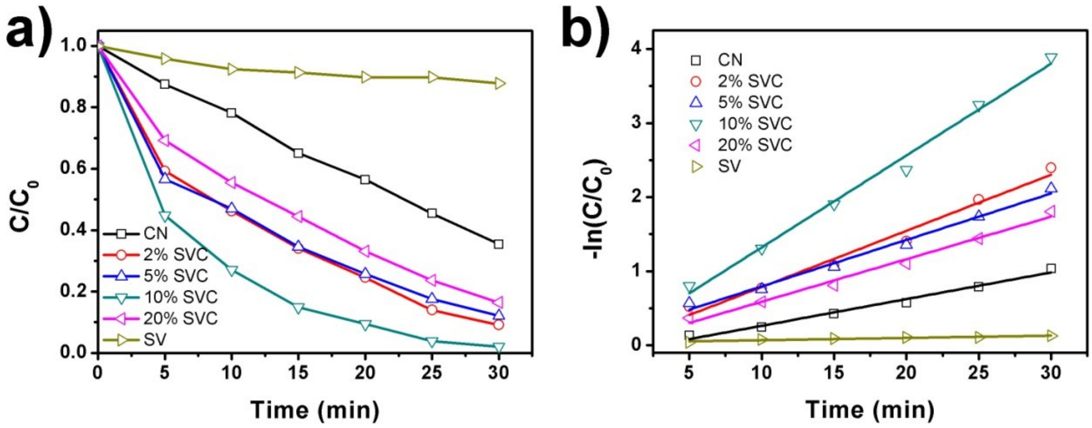

Fig. S8 Photocatalytic degradation of RhB over CN, SVCs and SV under visible light irradiation and b) corresponding first-order kinetics fitting plots

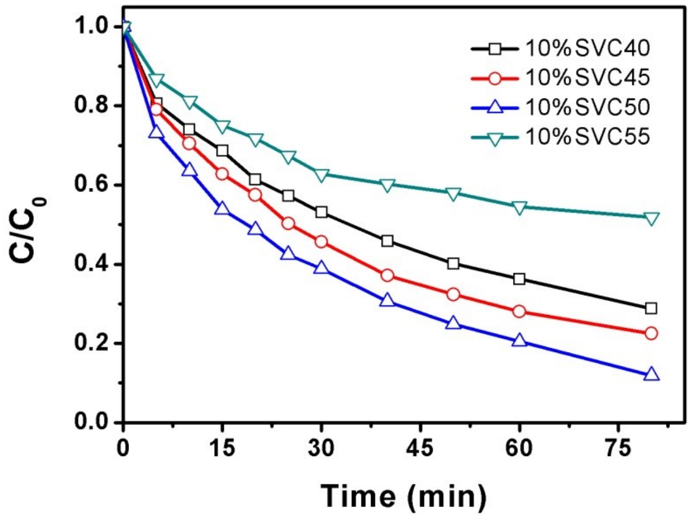

Fig. S9 Photocatalytic degradation of LVX over 10%SVC40, 10%SVC45, 10%SVC50, 10%SVC55

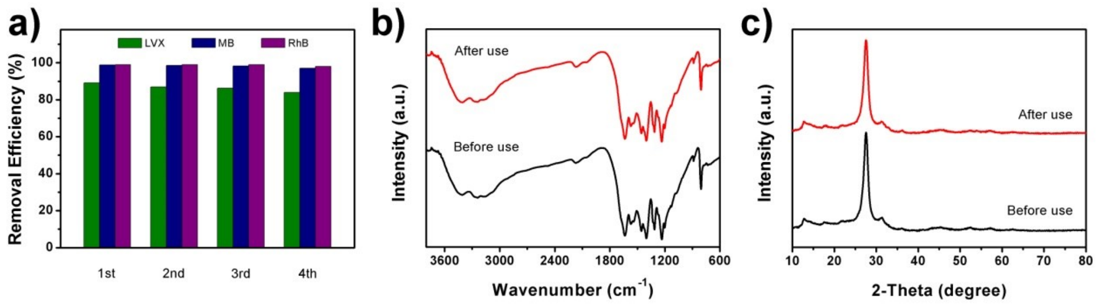

Fig. S10 a) Photocatalytic degradation of LVX, MB and RhB on 10%SVC over four cycles, b) FTIR spectra and c) XRD patterns of 10%SVC before and after the photodegradation reaction

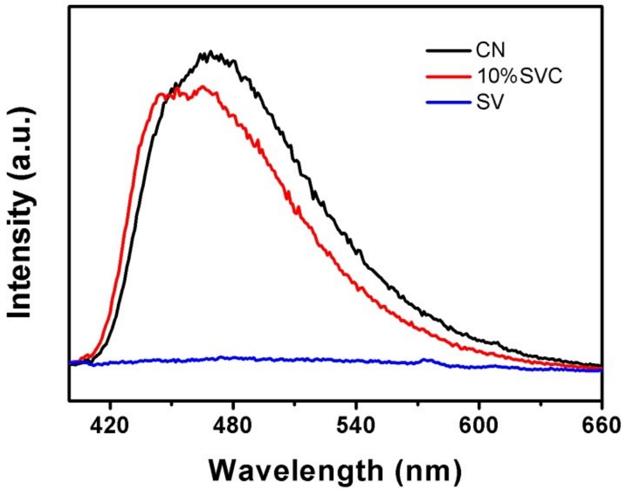

Fig. S11 PL spectra of CN, 10%SVC and SV

References

[1] F. Jiang, T. Yan, H. Chen, A. Sun, C. Xu, X. Wang, A g-C_3N_4–CdS composite catalyst with high visible-light-driven catalytic activity and photostability for methylene blue degradation. Applied Surface Science 2014, 295, 164–172.

[2] C. Xu, J. Wang, B. Gao, M. Dou, R. Chen, Synergistic adsorption and visible-light catalytic degradation of RhB from recyclable 3D mesoporous graphitic carbon nitride/reduced graphene oxide aerogels. J Mater Sci 2019, 54, 8892–8906.

[3] Z J.-Y. hang, J.-Y. Mei, S.-S. Yi, X.-X. Guan, Constructing of Z-scheme 3D g-C_3N_4-ZnO@graphene aerogel heterojunctions for high-efficient adsorption and photodegradation of organic pollutants. Applied Surface Science 2019, 492, 808–817.

[4] F. Chen, S. Huang, Y. Xu, L. Huang, W. Wei, H. Xu, H. Li, Novel ionic liquid modified carbon nitride fabricated by in situ pyrolysis of 1-butyl-3-methylimidazolium cyanamide to improve electronic structure for efficiently degradation of bisphenol A. Colloids and Surfaces A: Physicochemical and Engineering Aspects 2021, 610, 125648.

[5] Z. Jiao, Z. Liu, Z. Ma, Rodlike AgI/Ag2Mo2O7 Heterojunctions with Enhanced Visible-Light-Driven Photocatalytic Activity, ACS Omega 2019, 4, 7919−7930.

[6] Y. He, H. Lv, Y. Daili, Q. Yang, L.B. Junior, D. Liu, H. Liu, Z. Ma, Construction of a new cascade photogenerated charge transfer system for the efficient removal of bio-toxic levofloxacin and rhodamine B from aqueous solution: Mechanism, degradation pathways and intermediates study, Environ. Res. 187 (2020) 109647.

[7] H. Liu, M. Chen, H. Zhang, B. Wang, J. Peng, G. Liu, One-Step Synthesis of Hierarchical Flower-like SnO2/BiOCOOH Microspheres with Enhanced Light Response for the Removal of Pollutants, Langmuir 2020, 36, 9005−9013.

[8] A. Wang, H. Wang, H. Deng, S. Wang, W. Shi, Z. Yi, R. Qiu, K. Yan, Controllable synthesis of mesoporous manganese oxide microsphere efficient for photo-Fenton-like removal of fluoroquinolone antibiotics, Applied Catalysis B: Environmental 248 (2019) 298–308.